J. Nano- Electron. Phys.
3 (2011) No1, P.92-100

PACS numbers: 78.67.Bf, 75.75. + a, 61.72.uf

SYNTHESIS AND CHARACTERIZATION OF UNDOPED AND Co-DOPED SnO_2 NANOPARTICLES

R.N. Mariammal**, N. Rajamanickam, K. Ramachandran

School of Physics, Madurai Kamaraj University
Madurai – 21, India
* E-mail: marigayathrirn@yahoo.co.in

Undoped and Co-doped (1 and 3 at. %) SnO_2 nanoparticles were synthesized by a simple co-precipitation method. X-Ray diffraction data revealed that both undoped and doped samples crystallize in the tetragonal rutile phase with CoO phase in doped samples. The lattice parameters of doped samples calculated from XRD data do not vary much when compared to undoped one indicating that Co has not substituted the host lattice. The surface morphology investigated by SEM indicates the cluster formation in Co-doped (1 and 3 at. %) nanoparticles and the chemical composition of the samples were analyzed by energy dispersive spectroscopy (EDS). UV-Vis spectrum of undoped system showed absorption at 408 nm (3.04 eV), which is red shifted by 0.56 eV compared to bulk SnO_2 (3.6 eV) due to the cluster nature of the sample. The UV-Vis spectra of doped samples showed absorption in the visible region due to the formation of CoO phase, which is also evident from the XRD spectra. PL spectra showed characteristic UV emission at 409 nm and blue emission at 480 nm. The characteristic vibrational modes of SnO_2 were studied from FTIR analysis. EPR measurement of Co-doped (3 at .%) SnO_2 nanoparticles showed the paramagnetic behavior which may be attributed to the occupation of Co^{2+} ions in the interstitial site rather than the substitutional site. The absence of ferromagnetism is due to the high doping concentration of Co (> 1 at. %) and also due to the high annealing temperature which destroys the hyperfine splitting.

Keywords: *NANOPARTICLES, SEMICONDUCTORS, SCANNING ELECTRON MICROSCOPY, PHOTOLUMINESCENCE, MAGNETIC PROPERTIES.*

(Received 04 February 2011, in final form 18 March 2011)

1. INTRODUCTION

In recent years, diluted magnetic semiconductors (DMS) such as ZnO, TiO_2, and SnO_2 doped with transition metals (Co, Ni, V, Mn, Cr, and Fe) have attracted considerable interest due to their possibility of room temperature ferromagnetism (RTFM). Among these oxides, SnO_2 based DMS present special properties, such as giant magnetic moment and large coercivity [1]. SnO_2 is an n-type semiconducting oxide with a wide band gap of 3.6 eV. They have a wide range of applications in gas sensors [2, 3], optoelectronic devices [4], dye-sensitized solar cells [5], lithium batteries [6], and catalysts [7]. Many works reported RTFM in Co-doped SnO_2 nanoparticles. Still there are several controversies since some of the reports revealed the signature of paramagnetism and antiferromagnetism in these materials [8]. The oxygen stoichiometry plays an important role in RTFM in this system as reported by Punnose et al. [9]. Srinivas et al. [10] observed ferromagnetism in Co-doped (5 at.%) SnO_2 nanoparticles and found that the ferromagnetism increases

with increasing annealing temperature. They argued that the ferromagnetic properties are also attributed to the nanometric size of the materials in addition to the surface diffusion of Co ions and the distribution of defects such as oxygen vacancies or vacancy clusters. Punnose et al. [11] have discussed that uniform dopant distribution and annealing temperature play an important role in Co-doped SnO_2 nanoparticles for RTFM. Few reports showed that ferromagnetism disappears in Co-doped SnO_2 nanoparticles beyond a particular dopant concentration and annealing temperature [12]. In addition, the segregation of Co atoms on the surface of SnO_2 was also expected to destroy the RTFM [11]. Liu et al. [1] studied magnetism in Co-doped SnO_2 nanocrystals which showed antiferromagnetic behavior. Since many reports showed different results, here undoped and Co-doped (1 and 3 at. %) SnO_2 nanoparticles are synthesized, structurally and optically characterized in order to study the nature of magnetism in these samples.

2. EXPERIMENT

2.1 Synthesis

A simple co-precipitation method is adopted to synthesize undoped and Co-doped (1 and 3 at. %) SnO_2 nanoparticles. In a typical synthesis, tin (IV) chloride ($SnCl_4$) (0.1 M) was dissolved in 250 ml of de-ionized water and was magnetically stirred with drop wise addition of ammonia (NH_3) solution to maintain the pH of the solution at 7. Finally, the resultant solution was stirred constantly for 30 minutes. The obtained precipitate was centrifuged, washed several times with de-ionized water in order to remove the chloride and other unreacted ions, and then dried in atmosphere at 60 °C to get SnO_2 nanoparticles. Co doping (1 and 3 at. %) is achieved by adding appropriate amount of cobalt chloride ($CoCl_2.6H_2O$) to the SnO_2 stock solution. Finally, the nanoparticles obtained were annealed at 600 °C for 4 h in atmosphere to get undoped and Co-doped (1 and 3 at.%) SnO_2 nanoparticles. Flowchart for the synthesis of these nanoparticles is given in Fig. 1.

2.2 Characterization

The structural analysis of the synthesized nanoparticles was performed by recording the X-Ray diffraction (XRD) spectrum at room temperature using X-Ray diffractometer (PANalytical X'Pert Pro) with Cu-Kα as the radiation source (wavelength: 1.54056 Å) at a step size of 0.02° over the 2θ range of 10° to 90°. The morphology of the samples was examined by scanning electron microscopy (Hitachi S-3400N, Japan) operating at an accelerating voltage of 20 kV. The elemental analysis was carried out by energy dispersive spectroscopy (EDS) (Nortan System Six, Thermo electron corporation Instrument Super DRY II, USA). The UV-Vis absorption spectrum was recorded at room temperature using UV-Vis absorption spectrometer (Shimadzu). Fourier transform infrared (FT-IR) spectra were measured using the KBr method on a Fourier transform infrared spectrometer (Shiraz) at room temperature in the range of 4000 - 400 cm^{-1} with a resolution of 1 cm^{-1}. Photoluminescence (PL) studies were carried out using a photoluminescence spectrophotometer (Varian Cary Eclipse) and the spectra were recorded in the range of 375 - 680 nm using xenon flash lamp as the excitation source with an excitation wavelength of 350 nm.

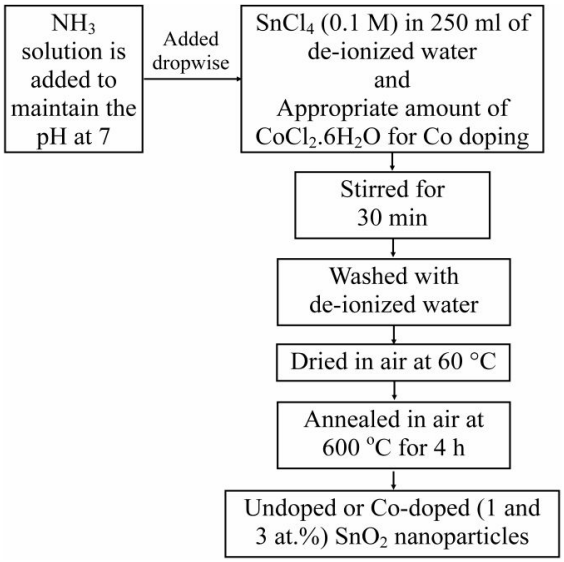

Fig. 1 *– Flowchart for the synthesis of undoped and Co-doped SnO_2 nanoparticles*

3. RESULTS AND DISCUSSION

3.1 X-Ray diffraction analysis

Fig. 2 shows the XRD spectra of undoped and Co-doped (1 and 3 at. %) SnO_2 nanoparticles. The spectra revealed that all the samples possess tetragonal rutile structure (JCPDS No. 41-1445). Eventhough Co-doped samples retain the rutile structure, they also show the presence of secondary phases of CoO.

Table 1 gives the lattice parameters of undoped and Co-doped SnO_2 nanoparticles. The lattice parameters of undoped SnO_2 nanoparticles are calculated from the XRD spectrum which are comparable with the JCPDS data and that of Co-doped samples do not show much variation compared to that of undoped one indicating that Co has not substituted the host lattice thus forming secondary phase of CoO, which is also evident from the appearance of extra peak corresponding to the hkl plane (002) of CoO in the XRD spectra of Co-doped samples. Also Co doping results in the broadening of the XRD peaks in the doped samples, which is due to the decrease in the crystallinity. Further by looking into the full width at half maximum of Bragg peaks, the average crystallite size of undoped and Co-doped SnO_2 nanoparticles is calculated from Scherrer's equation and is given in Table 1. The decrease in the crystallite size of doped samples when compared to undoped one is due to the decrease in the crystallinity of the doped samples.

Table 1 *– Results of XRD analysis on undoped and Co-doped (1 and 3 at. %) SnO_2 nanoparticles*

Samples	Crystallite size	*a* (Å)	*b* (Å)
SnO_2	12	4.70	3.18
SnO_2:Co (1 at.%)	9	4.71	3.18
SnO_2:Co (3 at.%)	8	4.69	3.18

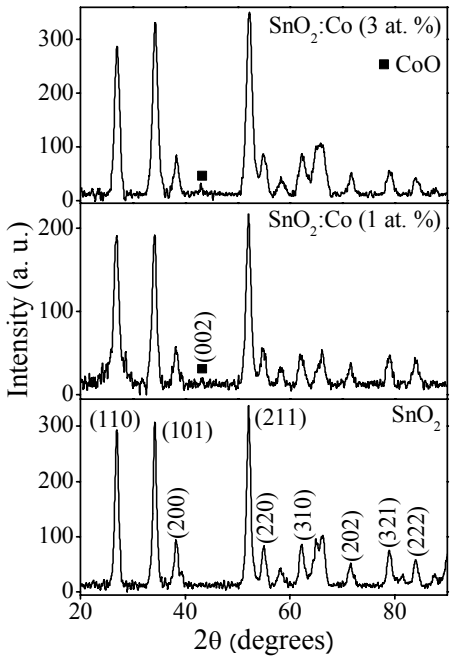

***Fig. 2** – XRD spectra of undoped and Co-doped (1 and 3 at. %) SnO_2 nanoparticles*

3.2 SEM analysis

The surface morphology of Co-doped (1 and 3 at.%) SnO_2 nanoparticles were studied by SEM analysis and the images are given in Fig. 3. The SEM images of both the samples show the formation of particles that agglomerated to form clusters. The cluster formation is due to annealing of the samples at 600 °C. Since SEM analysis is of low magnification, the individual particles are not clearly seen here. If we go for TEM analysis with high magnification, these particles can be clearly seen.

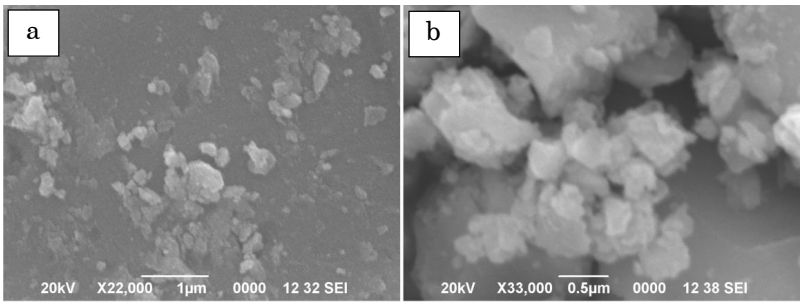

***Fig. 3** – SEM images of 1 at. % (a) and 3 at. % (b) Co-doped SnO_2 nanoparticles*

3.3 EDS analysis

The compositional analysis is necessary to monitor the concentration of the elements present in the sample. Fig. 4 (a and b) shows the typical EDS

spectra of Co-doped (1 and 3 at. %) SnO_2 nanoparticles which revealed signals from zinc, oxygen, and cobalt elements only with no other impurities. But the peak corresponding to Pt is obtained in the spectra since Pt is sprayed on the sample while taking SEM for conductivity. Table 2 shows the compositions of Co-doped (1 and 3 at. %) SnO_2 nanoparticles estimated from EDS analysis. Whenever a material is doped, it is necessary to see whether the dopant has entered the host system completely or partially. From the EDS analysis, it has been observed that the Co concentration in the doped samples is less than that of the starting solution. Even though we intended to dope 1 and 3 at. % of Co, only 0.31 and 0.65 at. % has actually entered the host system and the remaining less energetic molecules would be washed away during synthesis.

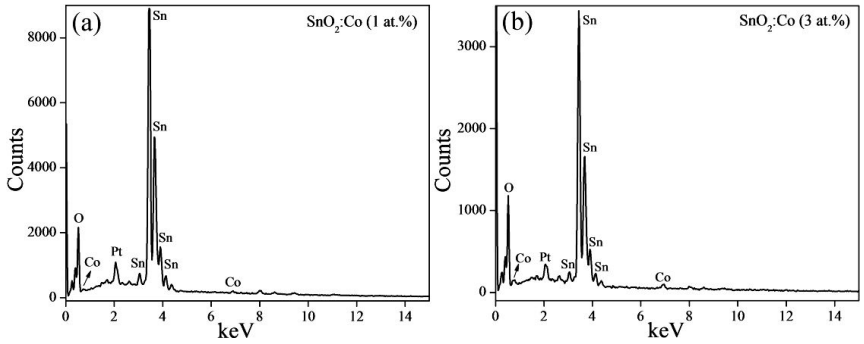

***Fig. 4** – EDS spectra of 1 at. % (a) and 3 at. % (b) Co-doped SnO_2 nanoparticles*

***Table 2** – The chemical compositions of Co-doped (1 and 3 at. %) SnO_2 nanoparticles*

Samples	Sn (at. %)	O (at. %)	Co (at. %)
SnO_2:Co (1 at.%)	21.45	78.23	0.31
SnO_2:Co (3 at.%)	15.99	83.36	0.65

3.4 UV-Vis analysis

The optical absorption spectra of undoped and Co-doped (1 and 3 at. %) SnO_2 nanoparticles are given in Fig. 5 and the spectrum of undoped sample shows absorption at 408 nm (3.04 eV) which is red shifted from the bulk (3.6 eV) due to the cluster nature of the sample. Co-doped samples do not exhibit a sharp absorption edge probably due to Co d states extending into the band gap region resulting from the overlapping of orbitals [10]. The absorption spectra of Co-doped samples also show visible absorption, which is due to the presence of CoO phase in these samples thus confirming that Co has not entered the host system.

3.5 Photoluminescence measurements

Fig. 6 shows the PL spectra of undoped and Co-doped (1 and 3 at. %) SnO_2 nanoparticles. PL measurements were carried out to understand the emission properties and the surface defects. Room temperature PL emission spectra of all the samples were recorded at an excitation wavelength of 350 nm which is in agreement with the reported value. The spectra show characteristic

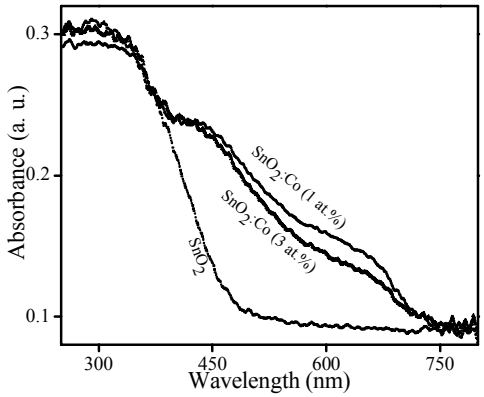

***Fig. 5** – UV-Vis absorption spectra of undoped and Co-doped (1 and 3 at.%) SnO_2 nanoparticles*

UV emission at 409 nm and this emission peak is due to all the luminescent centers, such as nanocrystals and intrinsic defects [13]. With the introduction of Co, the decrease in UV emission was attributed to the increased intrinsic defects of nanoparticles [13]. It is interesting to note that the emission spectral intensity of Co-doped (3 at. %) SnO_2 nanoparticles increases when compared to Co-doped (1 at. %) SnO_2 nanoparticles. This increased intensity is due to the decrease in the particle size as shown in Table 1 and this behavior may be attributed to an increase in the number of luminescence centers by increasing the ratio of surface area [10]. Apart from the UV emission, the spectra also show broad blue emissions at 480 and 492 nm that might be due to the electron transition mediated by defect levels in the band gap [13]. With the increase of Co concentration, the emission peaks broaden and this is mostly due to the decrease and non-uniformity of the particle size, which resembles with UV-Vis absorption studies.

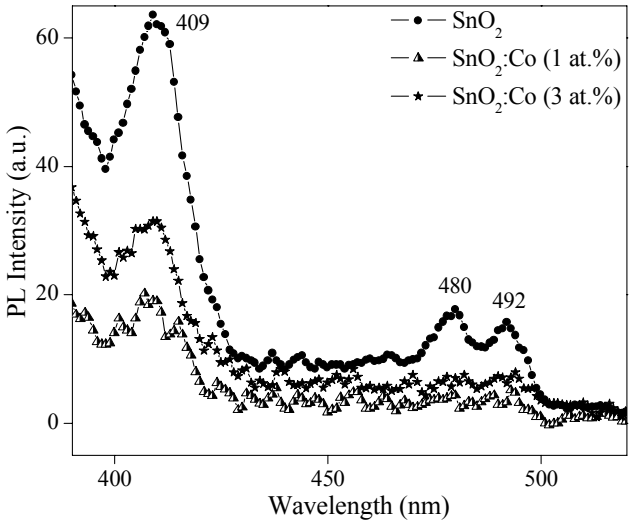

***Fig. 6** – PL spectra of undoped and Co-doped (1 and 3 at. %) SnO_2 nanoparticles*

3.6 FTIR analysis

Fig. 7 shows the FTIR spectra of the synthesized samples. The transmission band at 514 cm^{-1} is assigned to the Sn-O terminal bond of SnO_2 and that at 615 cm^{-1} is assigned to the O-Sn-O bridging bond [14]. The principal peak at 1629 cm^{-1} corresponds to the strong asymmetric stretching of C=O bond. The band observed at 2359 cm^{-1} is assigned to the existence of CO_2 molecule in air. Vibrational mode observed at 2923 cm^{-1} is due to C-H stretching vibration. The characteristic band at 3430 cm^{-1} corresponds to the stretching vibration of O–H groups.

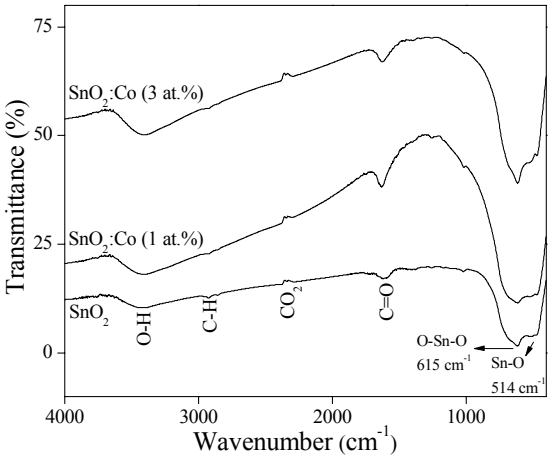

***Fig. 7** – FTIR spectra of undoped and Co-doped (1 and 3 at. %) SnO_2 nanoparticles*

3.7 EPR analysis

Fig. 8 shows the EPR spectrum of Co-doped (3 at. %) SnO_2 nanoparticles measured at room temperature. The spectrum resembles with the result obtained by Misra et al. [12]. They showed that this behavior is due to the incorporation of Co^{2+} ions with effective spin $S = 1/2$ in the interstitial site of SnO_2 nanoparticles. The expected hyperfine splitting terms corresponding to the ferromagnetism are not obtained here thus confirming the absence of ferromagnetism in this sample but exhibits a paramagnetic behavior [12]. Misra et al. [12] observed that the ferromagnetic behavior is lost when the doping concentration is greater than 1 at. % and also for samples annealed at temperature greater than 350 °C. Here the samples were annealed at 600 °C which may introduce randomly distributed defects as confirmed by PL emission spectra, which enhances disorder of the crystalline field at Co^{2+} sites, thereby increasing the hyperfine linewidth. Increasing the linewidth suppresses hyperfine splitting which further destroys the ferromagnetism. Also the SEM results showed the segregation of nanoparticles on the surface which is also responsible for the destruction of RTFM [11].

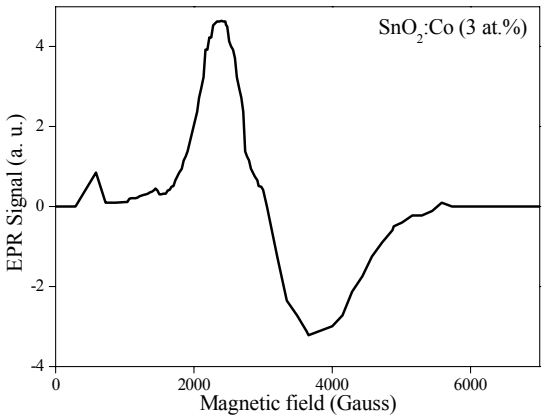

***Fig. 8** – EPR spectrum of Co-doped (3 at. %) SnO_2 nanoparticles*

Lande-g factor is calculated using

$$g = \frac{h\nu}{\mu_B H}, \tag{1}$$

where h is Planck constant, ν is the frequency, μ_B is the Bohr magneton, and H is the applied magnetic field in G. The value of g is found to be 2.819 for SnO_2:Co (3 at. %) nanoparticles.

4. CONCLUSION

Undoped and Co-doped (1 and 3 at.%) SnO_2 nanoparticles were synthesized by chemical co-precipitation method. The XRD analysis showed that the synthesized SnO_2 nanoparticles have tetragonal rutile structure and revealed the formation of secondary phase of CoO due to Co doping. The lattice parameters of doped samples do not vary much compared to undoped one. The appearance of CoO phase in the XRD spectra and the invariance of lattice parameters of doped samples confirmed that Co has not entered the substitutional site of the host system, which is further confimed by UV-Vis studies. The surface morphology and chemical composition were examined using SEM with EDS analysis. The absorption spectra of undoped sample showed absorption at 408 nm, which is red shifted from bulk and that of doped samples showed absorption in the visible region (due to CoO phase) without any sharp absorption peak. PL studies showed strong UV emission at 409 nm whose intensity decreased with the addition of Co which is due to the introduction of more intrinsic defects. Further, the vibrational modes were studied from FTIR analysis. EPR spectrum showed that Co-doped (3 at. %) SnO_2 nanoparticles exhibit paramagnetic behavior at room temperature.

ACKNOWLEDGEMENTS

The authors acknowledge DST Project on Nanotechnology and UGC-DRS & UPE for the financial support.

REFERENCES

1. C.M. Liu, X.T. Zu and W.L. Zhou, *J. Phys.: Condens. Matter* **18**, 6001 (2006).
2. Y. Wang, X. Jiang and Y. Xia, J. Am. *Chem. Soc.* **125**, 16176 (2003).
3. A.A. Firooz, A.R. Mahjoub and A.A. Khodadadi, *Sensor. Actuator. B* **141**, 89 (2009).
4. F. Gu, S.F. Wang, M.K. Lu, Y.X. Qi, G.J. Zhou, D. Xu and D.R. Yuan, *Opt. Mater.* **25**, 59 (2004).
5. S. Ferrere, A. Zaban and B.A. Gsegg, *J. Phys. Chem. B* **101**, 4490 (1997).
6. V. Subramanian, K.I. Gnanasekar and B. Rambabu, *Solid State Ionics* **175**, 181 (2004).
7. S.R. Stampfl, Y. Chen, J.A. Dumesis, Ch. Niu, C.G. Hill, *J. Catal.* **105**, 445 (1987).
8. A. Bouaine, N. Brihi, G. Schmerber, C.U. Bouillet, S. Colis and A. Dinia, *J. Phys. Chem. C* **111**, 2924 (2007).
9. A. Punnoose, J. Hays, V. Gopal and V. Shutthanandan, *Appl. Phys. Lett.* **85**, 1559 (2004).
10. K. Srinivas, M. Vithal, B. Sreedhar, M.M. Raja and P.V. Reddy, *J. Phys. Chem. C* **113**, 3543 (2009).
11. A. Punnoose, M.H. Engelhard and J. Hays, *Solid State Commun.* **139**, 434 (2006).
12. S.K. Misra, S.I. Andronenko, K.M. Reddy, J. Hays and A. Punnoose, *J. Appl. Phys.* **99**, 08M106 (2006).
13. M. Fang, X.T. Zu, Z.J. Li, S. Zhu, C.M. Liu, L.M. Wang and F. Gao, *J. Mater. Sci.: Mater. Electron* **19**, 868 (2008).
14. O.N. Gavrilenko, E.V. Pashkova and A.G. Belous, *Russ. J. Inorg. Chem.* **52**, 1835 (2007).